Individual variation of human $S1P_1$ coding sequence leads to heterogeneity in receptor function and drug interactions[S]

Hideru Obinata,* Sarah Gutkind,* Jeremiah Stitham,† Toshiaki Okuno,§ Takehiko Yokomizo,§ John Hwa,† and Timothy Hla[1,*]

Center for Vascular Biology,* Department of Pathology and Laboratory Medicine, Weill Cornell Medical College, Cornell University, New York, NY 10065; Yale Cardiovascular Research Center,† Section of Cardiovascular Medicine, Department of Internal Medicine, Yale University School of Medicine, New Haven, CT 06510; and Department of Biochemistry,§ Juntendo University School of Medicine, Tokyo 113-8421, Japan

Abstract Sphingosine 1-phosphate receptor 1 ($S1P_1$), an abundantly-expressed G protein-coupled receptor which regulates key vascular and immune responses, is a therapeutic target in autoimmune diseases. Fingolimod/Gilenya (FTY720), an oral medication for relapsing-remitting multiple sclerosis, targets $S1P_1$ receptors on immune and neural cells to suppress neuroinflammation. However, suppression of endothelial $S1P_1$ receptors is associated with cardiac and vascular adverse effects. Here we report the genetic variations of the $S1P_1$ coding region from exon sequencing of >12,000 individuals and their functional consequences. We conducted functional analyses of 14 nonsynonymous single nucleotide polymorphisms (SNPs) of the *S1PR1* gene. One SNP mutant (Arg^{120} to Pro) failed to transmit sphingosine 1-phosphate (S1P)-induced intracellular signals such as calcium increase and activation of p44/42 MAPK and Akt. Two other mutants (Ile^{45} to Thr and Gly^{305} to Cys) showed normal intracellular signals but impaired S1P-induced endocytosis, which made the receptor resistant to FTY720-induced degradation. Another SNP mutant (Arg^{13} to Gly) demonstrated protection from coronary artery disease in a high cardiovascular risk population. Individuals with this mutation showed a significantly lower percentage of multi-vessel coronary obstruction in a risk factor-matched case-control study.[H] This study suggests that individual genetic variations of $S1P_1$ can influence receptor function and, therefore, infer differential disease risks and interaction with $S1P_1$-targeted therapeutics.—Obinata, H., S. Gutkind, J. Stitham, T. Okuno, T. Yokomizo, J. Hwa, and T. Hla. **Individual variation of human $S1P_1$ coding sequence leads to heterogeneity in receptor function and drug interactions. *J. Lipid Res.* 2014.** 55: **2665–2675.**

Supplementary key words sphingosine phosphate • drug therapy • cell signaling • endocytosis • genetics • sphingosine 1-phosphate receptor • single nucleotide polymorphism

Sphingosine 1-phosphate receptor 1 ($S1P_1$) is a G protein-coupled receptor (GPCR) for a versatile lysophospholipid mediator sphingosine 1-phosphate (S1P) (1, 2). S1P levels are high in blood and lymph, but low in the interstitial tissue fluid, thereby forming a gradient important for immune cell trafficking (3). S1P, which is poorly soluble in aqueous solutions, is bound by specific chaperones. For example, plasma S1P is bound by albumin (4) or apoM (5), a specific apolipoprotein found in HDL. The S1P-$S1P_1$ signaling system is critical for sprouting angiogenesis (6–8) and vascular permeability (2, 9–11). In addition, part of the vasoprotective, anti-inflammatory, and anti-atherosclerotic effects associated with HDL is attributed to its cargo, apoM-S1P (12–15). The S1P-$S1P_1$ signaling system also plays an important role in immune cell trafficking (3). The gradient of S1P concentration between interstitial fluids and lymph is a basis that allows lymphocytes to egress from secondary lymphoid organs to the circulation via the chemotactic activity of $S1P_1$ (3, 16).

Previous studies have accumulated significant functional and structural information on $S1P_1$ (1, 2). The

This work was supported by National Institutes of Health Grants HL89934 and HL117798 to T.H., and the National Heart, Lung, and Blood Institute Grand Opportunity Exome Sequencing Project and its ongoing studies, which produced and provided exome variant calls for comparison: the Lung GO Sequencing Project (HL102923), the WHI Sequencing Project (HL102924), the Broad GO Sequencing Project (HL102925), the Seattle GO Sequencing Project (HL102926), and the Heart GO Sequencing Project (HL103010).

Manuscript received 22 August 2014 and in revised form 3 October 2014.

Published, JLR Papers in Press, October 7, 2014
DOI 10.1194/jlr.P054163

Abbreviations: CAD, coronary artery disease; FTY720, fingolimod/Gilenya; GFP, green fluorescent protein; GPCR, G protein-coupled receptor; HUVEC, human umbilical vein cord endothelial cell; NHLBI GO ESP, National Heart, Lung, and Blood Institute Grand Opportunity Exome Sequencing Project; SNP, single nucleotide polymorphism; S1P, sphingosine 1-phosphate; $S1P_1$, sphingosine 1-phosphate receptor 1; TEER, *trans*-endothelial electric resistance; UTR, untranslated region.

[1] To whom correspondence should be addressed.
e-mail: tih2002@med.cornell.edu

[S] The online version of this article (available at http://www.jlr.org) contains supplementary data in the form of text and four figures.

Copyright © 2014 by the American Society for Biochemistry and Molecular Biology, Inc.

This article is available online at http://www.jlr.org

recent crystal structure determination of $S1P_1$ has also enhanced our understanding of ligand interactions with the receptor (17, 18). Upon S1P binding, $S1P_1$ activates heterotrimeric $G\alpha_i$ protein and transmits signals via the p44/42 MAPK, PI3K/Akt, and Rac pathways (19–21). Subsequently, $S1P_1$ gets phosphorylated by GRK2 protein in the carboxyl terminal region (22) and undergoes clathrin-dependent endocytosis, then recycles back to the plasma membrane (23). This endocytosis/recycling pathway is essential for the regulation of $S1P_1$ activity. Impairment of the receptor endocytosis results in enhanced signaling and hyper-immune consequences, whereas vascular endothelial function is enhanced (24–26).

The study of the S1P-$S1P_1$ signaling system has entered the therapeutic era with the successful launch of fingolimod/Gilenya (FTY720) in the treatment of relapsing-remitting multiple sclerosis (27, 28). Indeed, many novel agonists and antagonists for $S1P_1$ have been developed and some of them are undergoing clinical trials to test their efficacy in the control of many diseases, including relapsing-remitting multiple sclerosis, the secondary progressive form of multiple sclerosis, psoriasis, and amyotrophic lateral sclerosis (29). Among them, FTY720, which gets phosphorylated into FTY720-P by sphingosine kinase-2 (10), induces irreversible ubiquitin-dependent degradation of $S1P_1$ and blocks lymphocyte egress from secondary lymphoid organs (25, 30). Genetic variations represented by single nucleotide polymorphisms (SNPs) confer individual variation in terms of susceptibility to certain diseases, development and severity of diseases, and efficacy and adverse effects of therapeutic drugs. However, our knowledge is quite limited on the genetic variations of $S1P_1$ and their effects on the receptor functions and disease development (31). Individual genetic variations of the *S1PR1* gene in various disease cohorts and their functional consequences may lead to a better understanding of $S1P_1$ biology in disease outcomes and in targeted therapeutics.

The National Heart, Lung, and Blood Institute Grand Opportunity Exome Sequencing Project (NHLBI GO ESP) sequenced protein-coding regions of the human genome across diverse, richly phenotyped populations with the ultimate aim to discover novel genes and mechanisms contributing to heart, lung, and blood disorders (32). The project has identified 14 nonsynonymous SNPs in the *S1PR1* gene out of more than 10,000 patients across many different clinical trials, with variations of the SNP prevalence from 1 to 0.001%. In this study, we determined the functional consequences of such nonsynonymous $S1P_1$ mutations. We also conducted a sequencing analysis of the *S1PR1* gene in a cardiovascular disease cohort with more than 1,800 patients in which we had access to clinical data including coronary angiograms. We report the identification of one loss-of-function mutation and two mutations that result in impaired receptor endocytosis. We also report one mutation that is associated with a significantly higher incidence in the cardiovascular disease cohort.

MATERIALS AND METHODS

Data collection from NHLBI GO ESP Exome Variant Server

Data for genetic variations of the *S1PR1* gene was collected from NHLBI GO ESP Exome Variant Server (32) according to the guidelines of the data usage. The data set was not linked to clinical phenotypes.

Cell culture

CHO-K1 and 293T cells were maintained in Ham's F-12 medium and DMEM (Sigma-Aldrich), respectively, containing 10% FBS. Human umbilical vein cord endothelial cells (HUVECs) were maintained on fibronectin-coated dishes in EGM2 medium (Lonza). Cells were cultured in a humidified 5% CO_2 incubator at 37°C.

Site-directed mutagenesis

cDNAs for $S1P_1$ mutants were generated using a QuikChange site-directed mutagenesis kit (Agilent). Primer information used for the mutagenesis is available in the supplementary material.

Lentivirus vectors and cell transduction

cDNAs for green fluorescent protein (GFP)-tagged WT and mutant $S1P_1$ were cloned in a pCDH-CMV-MCS-EF1-Puro vector (System Biosciences). A lentivirus vector for shRNA-mediated $S1P_1$ suppression was purchased from Sigma-Aldrich (the RNA Interference Consortium clone TRCN0000011359). Pseudoviral particles were made by transfecting these vectors together with packaging (pMDLg/pRRE and pRSV-Rev) and envelope (pMD2.G) plasmids into 293T producer cells. The culture supernatant containing pseudoviral particles was recovered and used to transduce cells. Transduced cells were selected by treatment with puromycin overnight.

Receptor endocytosis assay

Endocytosis of $S1P_1$ upon stimulation with S1P or FTY720-P was observed as described (33).

Western blot analysis

Cells were lysed by sonication in lysis buffer containing 50 mM Tris (pH 7.4), 100 mM NaCl, 1 mM EDTA, 1% Triton X-100, 0.5% Fos-Choline, 1 mM Na_3VO_4, 1 mM NaF, 10 mM β-glycerophosphate, and protease inhibitor cocktail (Sigma-Aldrich). Protein concentrations were determined by using a BCA protein assay kit (Thermo Scientific). Equal amounts of proteins were separated by SDS-PAGE, transferred to polyvinylidene difluoride membranes, and then probed with primary antibodies against total- and phospho-p44/42 MAPK (Cell Signaling #9102 and #9106, respectively), total- and phospho-Akt (Cell Signaling #9272 and #9271, respectively), $S1P_1$ (Santa Cruz #sc-25489), β-actin (Sigma-Aldrich #A5316), NA^+/K^+-ATPase (Developmental Studies Hybridoma Bank #α6F), and HRP-conjugated secondary antibodies. Signals were visualized by using Immobilon Western chemiluminescent HRP substrate (Millipore).

Cell-surface protein biotinylation assay

Cells were treated with a cell nonpermeable biotinylation reagent, EZ-link Sulfo-NHS-SS-Biotin (Thermo Scientific), and lysed in the lysis buffer. Biotinylated proteins were purified by using NeutrAvidin agarose beads (Thermo Scientific).

Measurement of intracellular calcium concentration

Changes in intracellular calcium concentrations upon ligand stimulation were monitored with a FLEX-station scanning fluorometer system (Molecular Devices) as described (34).

TABLE 1. Non-synonymous mutations of the human *S1PR1* gene found in the NHLBI GO ESP database

SNP Position	Identification Number (rs)	Alleles	EA Allele Number	AA Allele Number	Total Allele Number	cDNA Position	Protein Position	Amino Acid
1:101704572	rs61734752	A/C	A = 1/C = 7,019 (0.014%)	A = 163/C = 3,575 (4.36%)	A = 164/C = 10,594 (1.52%)	32	11	Asp/Ala
1:101704577	rs41287280	G/C	G = 116/C = 6,904 (1.65%)	G = 17/C = 3,721 (0.45%)	G = 133/C = 10,625 (1.24%)	37	13	Gly/Arg
1:101704655	rs140298731	A/G	A = 0/G = 7,020 (0%)	A = 1/G = 3,737 (0.027%)	A = 1/G = 10,757 (0.0092%)	115	39	Thr/Ala
1:101704674	rs148977042	C/T	C = 2/T = 7,018 (0.028%)	C = 2/T = 3,736 (0.054%)	C = 4/T = 10,754 (0.037%)	134	45	Thr/Ile
1:101704775	rs370003570	T/C	T = 0/C = 7,020 (0%)	T = 1/C = 3,737 (0.027%)	T = 1/C = 10,757 (0.0092%)	235	79	Ser/Pro
1:101704899	rs149198314	C/G	C = 1/G = 7,019 (0.014%)	C = 0/G = 3,738 (0%)	C = 1/G = 10,757 (0.0092%)	359	120	Pro/Arg
1:101705133	rs370425078	G/A	G = 0/A = 7,020 (0%)	G = 1/A = 3,737 (0.027%)	G = 1/A = 10,757 (0.0092%)	593	198	Cys/Tyr
1:101705252	rs149041375	T/C	T = 2/C = 7,018 (0.028%)	T = 1/C = 3,737 (0.027%)	T = 3/C = 10,755 (0.028%)	712	238	Cys/Arg
1:101705274	rs151135641	A/G	A = 0/G = 7,020 (0%)	A = 1/G = 3,737 (0.027%)	A = 1/G = 10,757 (0.0092%)	734	245	Asn/Ser
1:101705453	rs146890331	T/G	T = 1/G = 7,019 (0.014%)	T = 0/G = 3,738 (0%)	T = 1/G = 10,757 (0.0092%)	913	305	Cys/Gly
1:101705535	rsrs7549921	G/C	G = 0/C = 7,020 (0%)	G = 2/C = 3,736 (0.054%)	G = 2/C = 10,756 (0.019%)	995	332	Arg/Pro
1:101705565	rs138199836	C/G	C = 2/G = 7,018 (0.028%)	C = 0/G = 3,738 (0%)	C = 2/G = 10,756 (0.019%)	1,025	342	Pro/Arg
1:101705579	rs375635245	A/G	A = 1/G = 7,019 (0.014%)	A = 0/G = 3,734 (0%)	A = 1/G = 10,753 (0.0092%)	1,039	347	Ser/Gly
1:101705591	rs149581242	G/A	G = 0/A = 7,010 (0%)	G = 1/A = 3,735 (0.027%)	G = 1/A = 10,745 (0.0093%)	1,051	351	Cly/Ser

The allele numbers in the European American (EA allele) and African American (AA allele) population are shown, as well as the total allele number as of June 2012.

Collection of patient samples and sequencing analysis of the *S1PR1* gene

Patients were recruited from Dartmouth-Hitchcock Medical Center under a protocol approved by the Institutional Review Board (35). Genomic DNA was extracted from blood using a PuregeneH system (Gentra Systems). The coding sequence of the human *S1PR1* gene was amplified by PCR using the human genomic DNAs as templates and the following primers: 5′-tctccagccaaggaaaagc-3′ and 5′-agtaaagagcgcttccgg-3′. The amplified DNAs were purified using a QIAquick PCR purification kit (Qiagen) and subjected to Sanger DNA sequencing analyses at the Genomics Facility of the Biotechnology Resource Center, Cornell University.

Human HDL preparation

Lipoprotein particles with the density ranging from 1.066 to 1.21 were collected from human plasma by repeated ultracentrifugation as described (36), and dialyzed against PBS. S1P concentration contained in the HDL fraction was determined by a

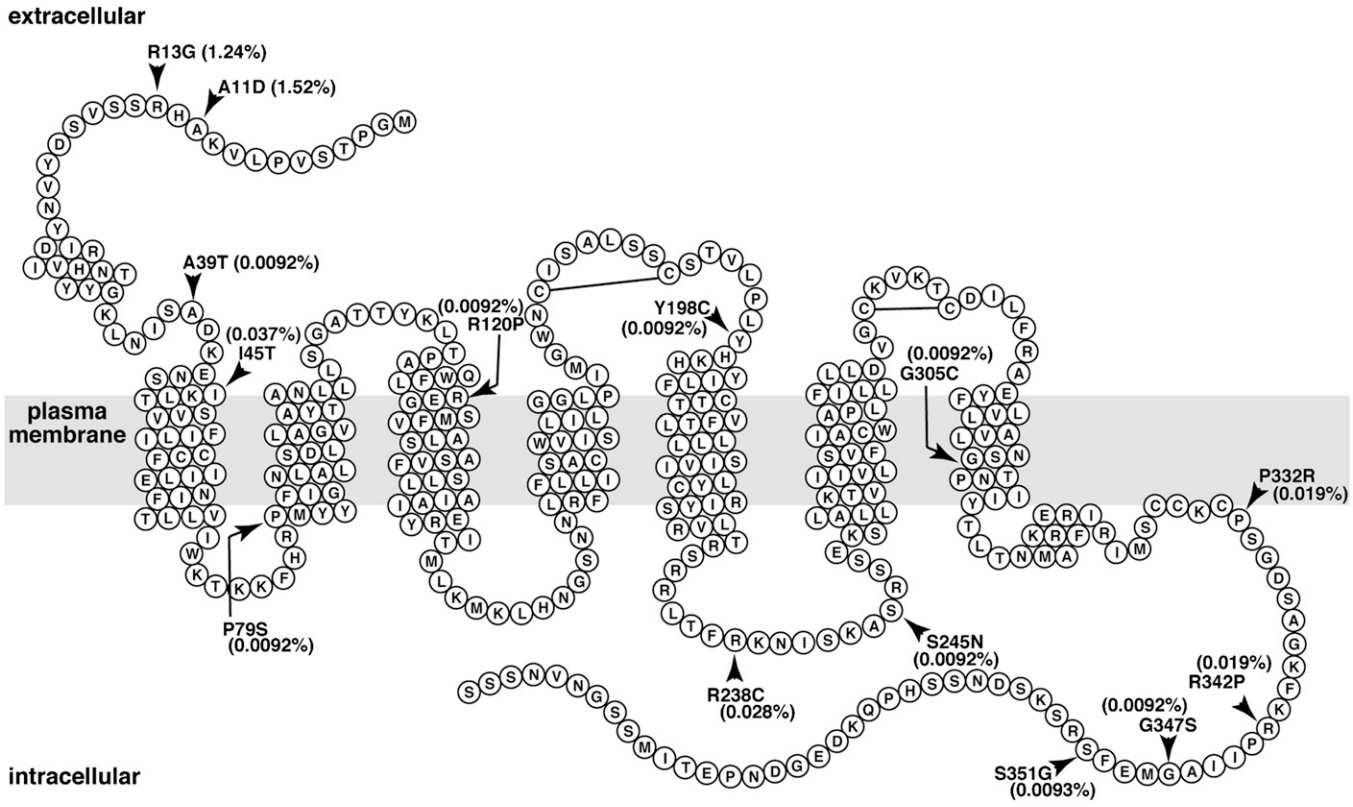

Fig. 1. Serpentine diagram of the secondary structure of human $S1P_1$. Each circle represents one amino acid residue with a one letter amino acid code. The gray rectangle represents the plasma membrane. Positions of α-helixes were determined by referring the crystal structure of $S1P_1$ (Protein Data Bank number 3V2Y) and by using a hydrophobicity-calculation program, SOSUI. Arrowheads denote the positions of amino acids changed in the 14 nonsynonymous mutations in the NHLBI GO ESP database. Prevalence of the 14 mutations is shown as percent of total sample numbers. Two extracellular disulfide bonds are also shown.

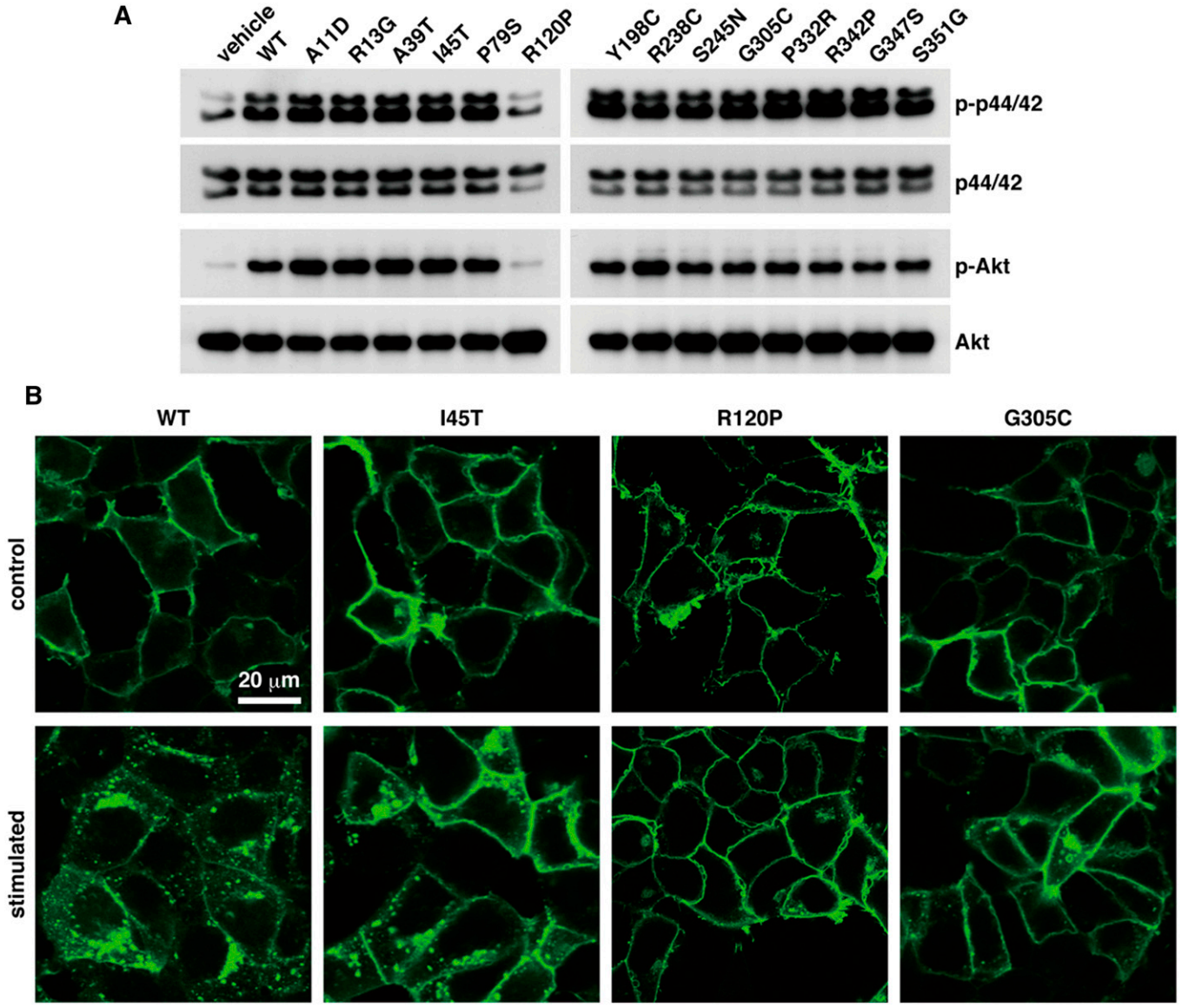

Fig. 2. Characterization of 14 SNP mutants found in the NHLBI GO ESP database. CHO-K1 (A) or 293T (B) cells were transduced with lentivirus vectors for the expression of GFP-tagged $S1P_1$ mutants, starved overnight, and then stimulated with 100 nM S1P for 5 min (A) or 200 nM S1P for 1 h (B). A: Total cell lysates were prepared and subjected to Western blot analyses for the activation of p44/42 MAPK and Akt. B: The cells were fixed with paraformaldehyde, and the GFP signal was observed for the localization of the $S1P_1$ mutants under a confocal microscope system. Data are representative of at least three independent experiments with the same tendency.

LC-MS/MS analysis in the Lipidomics Shared Resources at the Medical University of South Carolina (37).

Measurement of *trans*-endothelial electric resistance

HUVECs were seeded onto gelatin-coated gold electrodes (8W10E plates, Applied BioPhysics), serum starved in EBM2 medium (Lonza) for 1 h, and stimulated with S1P. Endothelial barrier function was assessed by monitoring electric resistance of the electrodes with an ECIS θ system (Applied BioPhysics).

RESULTS

Genetic variations of the *S1PR1* gene found in the NHLBI GO ESP database

To examine the genetic variations of the *S1PR1* gene, we performed a database search in the NHLBI GO ESP database (32). As of June 2012, we found 33 SNPs in the *S1PR1* gene, consisting of 14 nonsynonymous mutations (**Table 1**), 14 synonymous mutations, 4 mutations in the 5′-untranslated region (UTR), and 1 mutation in the 3′-UTR. The positions of the amino acids changed in the 14 nonsynonymous mutations are illustrated in the secondary structure of $S1P_1$ (**Fig. 1**). Those include Ala^{11} to Asp (A11D), R13G, A39T, I45T, P79S, R120P, Y198C, R238C, S245N, G305C, P332R, R342P, G347S, and S351G. Among them, A11D and R13G show relatively higher prevalence (>1%) in the African American and European American populations, respectively (Table 1).

Functional analysis of the $S1P_1$ SNP mutants

We expressed $S1P_1$ harboring each mutation in CHO-K1 cells, and stimulated the cells with the ligand S1P to test

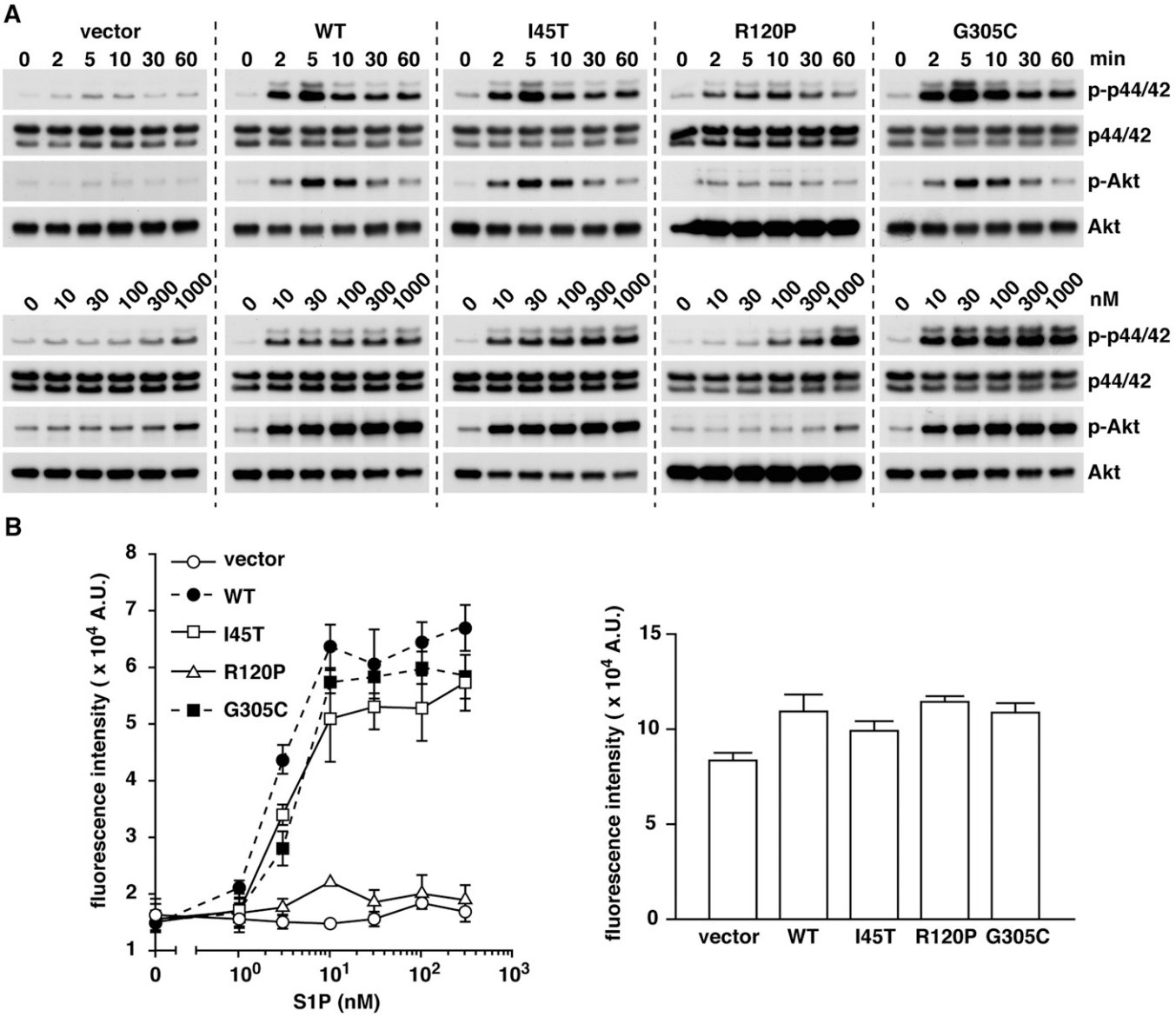

Fig. 3. Comparison of WT $S1P_1$ with I45T, R120P, and G305C mutants. A: The CHO-K1 cells expressing each receptor were serum starved overnight and stimulated with 100 nM S1P for the indicated times (upper panel) or with the indicated concentrations of S1P for 5 min (lower panel). Data are the representative of two independent experiments with the same tendency. B (left): The cells were loaded with a calcium-sensitive fluorescent dye, fluo-8 AM. The changes in intracellular calcium concentration upon exposure to S1P were analyzed by a FlexStation system. Data represent the mean ± SEM (n = 3). B (right): The cells were also stimulated with a positive control ATP (10 μM) to check the similar fluo-8 loading efficiency and the cell viability. Data are representative of three independent experiments with the same tendency.

the ability of the SNP mutations to influence the receptor-mediated activation of p44/42 MAPK and Akt signaling proteins. As shown in **Fig. 2A**, R120P mutant failed to mediate the activation of p44/42 MAPK and Akt in response to 100 nM S1P, while the other mutants did not show any change compared with WT $S1P_1$. Arg^{120} is a critical residue for the binding of S1P through the interaction of its basic side chain with the phosphate group of S1P (17, 38). S1P binding ability of the receptor was largely impaired by R120A mutation (38). Thus, the defect of the R120P mutant in S1P-induced signaling is likely due to impaired S1P binding ability.

We also examined ligand-induced receptor endocytosis that is an important step for the receptor desensitization processes (23). All of the mutants showed cell surface localization after serum starvation in the same way as WT $S1P_1$ (Fig. 2B, supplementary Fig. I), which indicates that none of the mutations affect receptor translation and trafficking to the plasma membrane in the basal condition. Upon S1P stimulation, R120P mutant showed no receptor endocytosis (Fig. 2B), which confirms that activation of the receptor by S1P is impaired in the R120P mutant. Surprisingly, I45T showed diminished endocytosis and G305C failed to undergo endocytosis upon S1P stimulation (Fig. 2B). All other mutants responded to S1P and endocytosed in an indistinguishable manner from the WT (supplementary Fig. I).

We further explored the time course and ligand-dose dependency of p44/42 and Akt activation in CHO-K1 cells

overexpressing WT $S1P_1$, I45T, R120P, and G305C mutants. We confirmed a similar level of expression of each receptor (supplementary Fig. II). As shown in **Fig. 3A**, I45T did not show any differences compared with WT $S1P_1$ both in the time course and dose dependency. G305C had overall similar, but slightly enhanced, signaling compared with WT $S1P_1$, which could be due to the defect in endocytosis-mediated desensitization processes (Fig. 2B). A higher dose of S1P (>100 nM) did induce modest activation of p44/42 MAPK in cells expressing the R120P mutant. This indicates that the R120P mutant is not completely insensitive to S1P, suggesting that several other residues, such as Tyr^{29}, Lys^{34}, Asn^{101}, and Glu^{121}, also contribute to the recognition of the head group of S1P (17). We also measured the increase in intracellular calcium concentration that is a proximal downstream event of the receptor activation. I45T and G305C mutants did not show any differences from WT $S1P_1$, but the R120P mutant failed to mediate the calcium response (Fig. 3B). These results show that I45T and G305C mutants maintain the normal properties in the receptor activation but the receptor desensitization processes are impaired, while the R120P mutant shows largely impaired receptor activation.

Diminished efficacy of FTY720 on I45T and G305C mutants

Endocytosis of $S1P_1$ plays an important role in the receptor desensitization. It is a crucial process in the regulation of lymphocyte trafficking. In circulating lymphocytes, $S1P_1$ is internalized in response to high concentrations of S1P in blood and lymph. In secondary lymphoid organs, S1P concentrations are maintained low, thus $S1P_1$ recovers its cell surface localization (3). This is the basis for enabling lymphocytes to egress from lymphoid organs toward circulation along the gradient of S1P concentration. FTY720 inhibits the egress of lymphocytes from secondary lymphoid organs by inducing internalization and irreversible $S1P_1$ degradation in the proteasome (25, 30). Recently, our group showed that mutant mice harboring the *S1PR1* gene encoding phosphorylation-deficient, and as such endocytosis-deficient, receptors [$S1P_1$ (S5A)] developed severe experimental autoimmune encephalomyelitis due to T helper 17 cell-mediated autoimmunity, both in the peripheral immune system and the nervous system (26). This $S1P_1$ (S5A) receptor shows resistance to FTY720-induced degradation both in vivo and in vitro (25, 30).

The defect in the endocytosis response found in I45T and G305C mutants phenocopies the $S1P_1$ (S5A) receptor and may also lead to the resistance to FTY720-induced endocytosis and degradation. We examined the efficacy of FTY720-P, a phosphorylated form of FTY720, on I45T and G305C mutants, and found that these mutants showed much weaker endocytosis in response to FTY720-P treatment compared with the strong internalization of WT $S1P_1$ (supplementary Fig. III). As a consequence of diminished endocytosis, I45T and G305C mutants showed much less FTY720-induced degradation than WT $S1P_1$ (**Fig. 4A**). To confirm quantitatively that the endocytosis response is impaired in I45T and G305C mutants, we measured cell surface $S1P_1$ before and after FTY720-P treatment. As shown in Fig. 4B, C, WT $S1P_1$ showed a 56% decrease in the cell surface amount after 1 h of FTY720-P treatment, while I45T and G305C showed only 16 and 13% decreases, respectively. These results suggest that the efficacy of FTY720 treatment could be impaired in individuals who carry these genetic variations in the *S1PR1* gene.

Sequencing analysis and phenotype correlation of the *S1PR1* gene in a cardiovascular cohort

The S1P-$S1P_1$ signaling system also plays an important role in vascular development and homeostasis. Dysfunction of this system leads to increased vascular permeability and hypersensitivity to anaphylactic stimulus (2, 9–11). Anti-inflammatory effects of HDL on the endothelium are partially attributed to its cargo S1P (12–15). Moreover, one of the adverse effects of FTY720 in therapeutics for multiple sclerosis is bradycardia, which is associated with the agonistic effects of FTY720 on $S1P_1$ and subsequent activation of the G protein-coupled inwardly rectifying potassium channel in cardiomyocytes (39). Therefore, it is of clinical

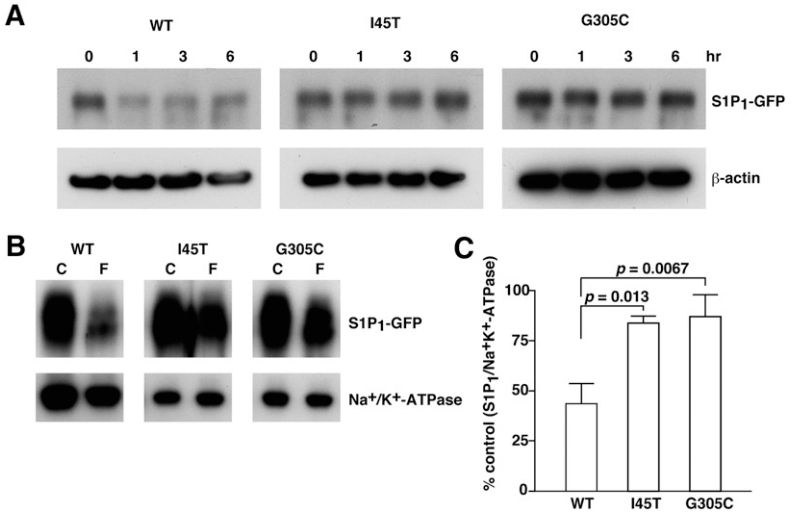

Fig. 4. Diminished efficacy of FTY720-P on I45T and G305C mutants. CHO-K1 cells were transduced with lentivirus vectors for the expression of GFP-tagged $S1P_1$, I45T, and G305C, starved overnight, and then stimulated with 10 nM FTY720-P for the indicated time (A) or for 1 h (B). A: Total cell lysates were prepared and subjected to Western blot analyses for the degradation of $S1P_1$. B: Cell-surface proteins were biotinylated, purified, and subjected to Western blot analyses to check the amount of $S1P_1$ remaining on the cell surface after FTY720-P treatment. C: Densitometric analysis of (B) using the National Institutes of Health ImageJ program is shown. Data represent the mean ± SD (n = 3).

TABLE 2. Non-synonymous mutations of the human *S1PR1* gene found in the sequence analysis of 1,814 patients of the cardiovascular cohort

Alleles	Allele Number	cDNA Position	Protein Position	Amino Acid
A/C	A = 1/C = 1,813 (0.055%)	32	11	Asp/Ala
G/C	G = 65/C = 1,749 (3.58%)	37	13	Gly/Arg
A/G	A = 1/G = 1,813 (0.055%)	58	20	Ile/Val
T/C	T = 1/C = 1,813 (0.055%)	712	238	Cys/Arg
A/C	A = 1/C = 1,813 (0.055%)	999	333	Arg/Ser

Sample number analyzed = 1,814.

importance to examine the prevalence of nonsynonymous mutations in the *S1PR1* gene in a cardiovascular disease cohort and its relationship with disease severity or with sensitivity to FTY720. Toward this end, we performed a sequencing analysis of the *S1PR1* gene in 1,814 patients in a high cardiovascular risk population (35). As summarized in **Table 2**, we found five nonsynonymous mutations that resulted in amino acid changes of A11D, R13G, V20I, R238C, and S333R. The mutations for V20I and S333R have not been reported before. R13G showed a significantly higher incidence than that observed in the NHLBI GO ESP (3.58% versus 1.24%). The other detected mutations were rare (0.0055%). Because coronary angiograms (for detection of coronary obstruction) were available on all the patients, we compared the R13G patients (n = 59) to age- and risk factor-matched control patients (n = 236 in a 4:1 match). R13G appeared to protect from coronary artery disease (CAD); significantly more patients had no CAD and significantly fewer patients had multiple vessel obstruction compared with the control patients (**Table 3**, **Fig. 5**).

Functional analysis of the R13G mutation of $S1P_1$ in endothelial cells

R13G mutation was enriched in the high cardiovascular risk population, but appeared to protect from CAD. To understand this apparent discrepancy, we examined functional differences of the R13G mutant in endothelial cells. GFP-tagged WT $S1P_1$ or R13G mutant were overexpressed in HUVECs with endogenous $S1P_1$ knocked-down by specific shRNA against 3′-UTR of $S1P_1$ (**Fig. 6A**). These cells were stimulated with an increasing dose of HDL prepared from human plasma (S1P concentration from 1 to 100 nM) to check activation of p44/42 MAPK and Akt. As shown in Fig. 6B, C, R13G mutant did not show any significant differences from WT $S1P_1$. We also measured changes in *trans*-endothelial electric resistance (TEER) upon S1P stimulation in these HUVECs, because one of the important functions of $S1P_1$ in endothelial cells is strengthening adherens junctions to maintain vascular barrier integrity (9, 40). HDL-bound S1P increased the TEER in a dose-dependent manner, and the R13G mutant did not show any difference from WT $S1P_1$ (Fig. 6D, upper). The same tendency was observed when these cells were stimulated with BSA-bound S1P (Fig. 6D, lower). Thus, we did not find detectable difference of the R13G mutant in endothelial cells, at least in the assay systems we performed, though the cohort analysis of cardiovascular patients showed that patients with the R13G mutant had a significantly lower incidence of multi-vessel obstructions. We also examined the effects of I45T and G305C mutations on the S1P-induced increases in TEER, but did not find any differences compared with the WT receptor (supplementary Fig. IV).

TABLE 3. Age-, gender-, and risk factor-matched case-control comparison between R13G and WT $S1P_1$

Factor	R13G (n = 59)	WT (n = 236)	Significance
Age (± SEM)[a]	66.49 ± 1.51	66.80 ± 0.83	NS
Male (% total)[a]	41 (69.5%)	165 (69.9%)	NS
Female (% total)[a]	18 (30.5%)	71 (30.1%)	NS
BMI (± SEM)[a]	29.37 ± 0.76	29.03 ± 0.42	NS
HTN (% total)[a]	40 (67.8%)	163 (69.1%)	NS
Chol (% total)[a]	46 (77.9%)	179 (75.8%)	NS
FHx (% total)[a]	26 (44.1%)	103 (43.6%)	NS
DM (% total)[a]	23 (38.9%)	98 (41.5%)	NS
Smoking (% total)[a]	9 (15.2%)	33 (14.0%)	NS
LM (% total)[b]	26 (44.1%)	105 (44.5%)	NS
LAD (% total)[b]	50 (84.7%)	212 (89.8%)	NS
LCx (% total)[b]	46 (77.9%)	200 (84.7%)	NS
RCA (% total)[b]	49 (83.0%)	207 (87.7%)	NS
Multivessel disease (% total)[b]	49 (83.0%)	219 (93.2%)	$P < 0.05$
Number of diseased vessels (± SEM)[b]	2.98 ± 0.17	3.07 ± 0.06	NS
Number of cardiovascular events (± SEM)[b]	1.89 ± 0.20	1.78 ± 0.78	NS
Number of post interventions (± SEM)[b]	0.57 ± 0.07	0.62 ± 0.04	NS

HTN, hypertension; Chol, dyslipidemia; FHx, family history of cardiovascular diseases; DM, diabetes mellitus; LM, left main coronary artery; LAD, left anterior descending coronary artery; LCx, left circumflex coronary artery; RCA, right coronary artery.

[a]Age, gender and risk factors were matched between the case (R13G mutant, n = 59) and the control (WT $S1P_1$, n = 236).

[b]Numbers of patients with no CAD and with multivessel disease (obstruction in >1 major coronary artery) are shown.

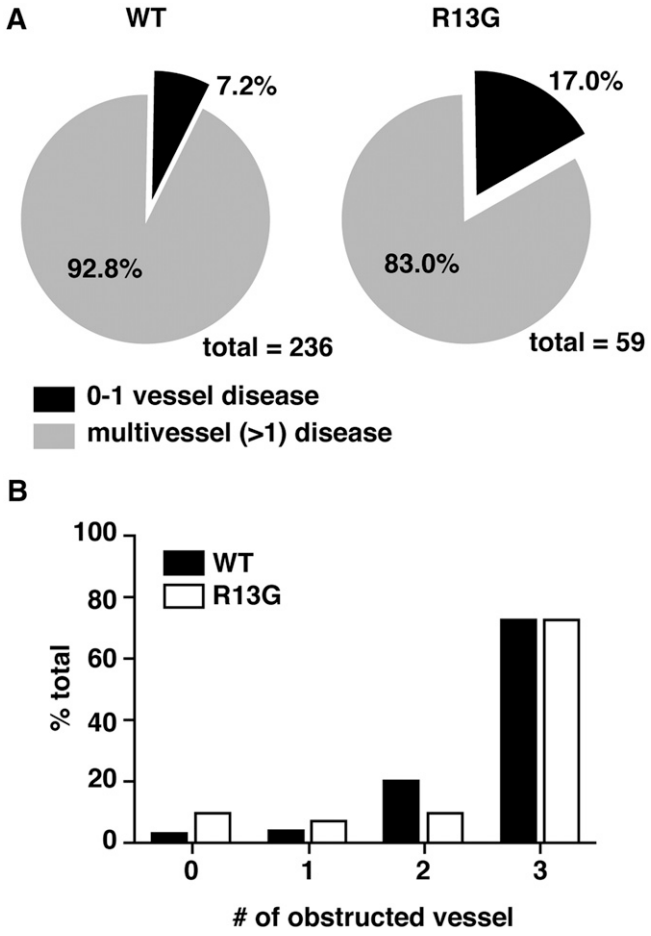

Fig. 5. Lower percentage of multi-vessel obstructions in the patients with R13G mutation. A: A pie chart shows the percentages of the patients with zero or one (black) or with two or more (gray) obstructed vessels observed in coronary angiography in the case-control study between the R13G mutant and WT $S1P_1$. B: Distribution of the obstructed vessel number is shown.

DISCUSSION

In this study, we characterized 14 nonsynonymous mutations of $S1P_1$ found in the NHLBI GO ESP database. We found three mutations that showed functional differences; R120P showed a defect in both ligand-induced activation and endocytosis, while I45T and G305C only showed a defect in ligand-induced endocytosis. These three residues are all located in the transmembrane helixes in sharp contrast to the other 11 mutations in the extra- or intracellular region (Fig. 1, and **Fig. 7**), which suggests that nonsynonymous mutations in transmembrane helixes of GPCRs tend to result in functional alterations. R120P is a loss-of-function mutation and can be a risk factor for various diseases, considering a pivotal role of the S1P-$S1P_1$ signaling system in cardiovascular and immune systems. Because the $S1P_1$ knockout mouse is embryonic lethal at around E12.5 due to defects in vascular development (41, 42), homozygotes for the R120P mutation are most likely embryonic lethal. Effects of heterozygous loss-of-function of $S1P_1$ should be explored in mouse disease models and/or in various cohort studies.

I45T and G305C showed attenuated ligand-induced endocytosis/degradation, though they mediate intracellular signaling normally. I45T and G305C mutants phenocopy a $S1P_1$ (S5A) mutant in which five serine residues in the carboxyl-terminal region are substituted with alanine. Recently, our group reported that $S1P_1$ (S5A) mutant mice showed enhanced autoimmunity and developed severe experimental autoimmune encephalomyelitis (26). Thus, impairment of the receptor internalization in I45T and G305C mutants may result in increased autoimmunity as observed in $S1P_1$ (S5A) mice, raising a possibility that these SNPs can be potential risk factors for autoimmune diseases. In multiple sclerosis patients, these two SNPs would hamper the ability of FTY720 treatment to induce degradation of $S1P_1$. It is of clinical importance to explore the prevalence of I45T and G305C mutations and their involvement in disease development in several autoimmune disease cohorts.

In contrast to the established importance of Arg^{120} in S1P binding (17, 38), no clear function has been attributed to Ile^{45} and Gly^{305} so far. Substitution of Ile^{45} to Thr results in an amino acid sequence of $Asn^{43}Ser^{44}Thr^{45}$, which makes a potential N-linked glycosylation site (N-X-S/T). N-linked glycosylation of transmembrane proteins, including GPCRs, occurs in the endoplasmic reticulum and plays roles in proper folding and trafficking to the cell surface (43). Most GPCRs have one or more N-linked glycosylation sites in the extracellular domain (44), though the functions of N-linked glycosylation have not been well-clarified. The I45T mutant of $S1P_1$ showed normal localization on the cell surface and ligand-induced activation of intracellular signaling pathways, which means this mutation does not affect proper folding of the receptor and trafficking to the cell surface. In mouse $S1P_1$, which has one N-linked glycosylation site in the N-terminal region, mutation of this Asn resulted in poor association with caveolae and impaired ligand-induced endocytosis (45). A similar defect in ligand-induced endocytosis by a nonglycosylated mutant was observed in protease-activated receptor 1 (46). Thus, glycosylation of the extracellular region of GPCRs is somehow involved in the regulation of ligand-induced endocytosis in some cases. Human $S1P_1$ has two putative N-linked glycosylation sites (Asp^{30} and Asp^{36}) in the close vicinity of Asp^{43}, though glycosylation of these residues has not been confirmed. Additional glycosylation of Asp^{43} might interfere with functions of these putative glycosylated residues. Because Ile^{45} is located in the beginning of transmembrane helix I and faces the ligand-binding pocket, as illustrated in Figs. 1 and 7, another possibility is that the I45T mutation and/or glycosylation of Asp^{43} interferes with ligand-induced conformational changes of the receptor necessary for internalization responses.

G305C shows an even more severe defect in the endocytosis than I45T. Gly^{305} is located in the middle of transmembrane helix VII (Figs. 1, 7). A stretch of polar amino acids with a glycine in the middle ($Asn^{303}Ser^{304}Gly^{305}Thr^{306}Asn^{307}$) precedes a highly conserved NPXXY motif and makes the helix VII loose, allowing some flexibility of this transmembrane region (Fig. 7). Glycine is energetically

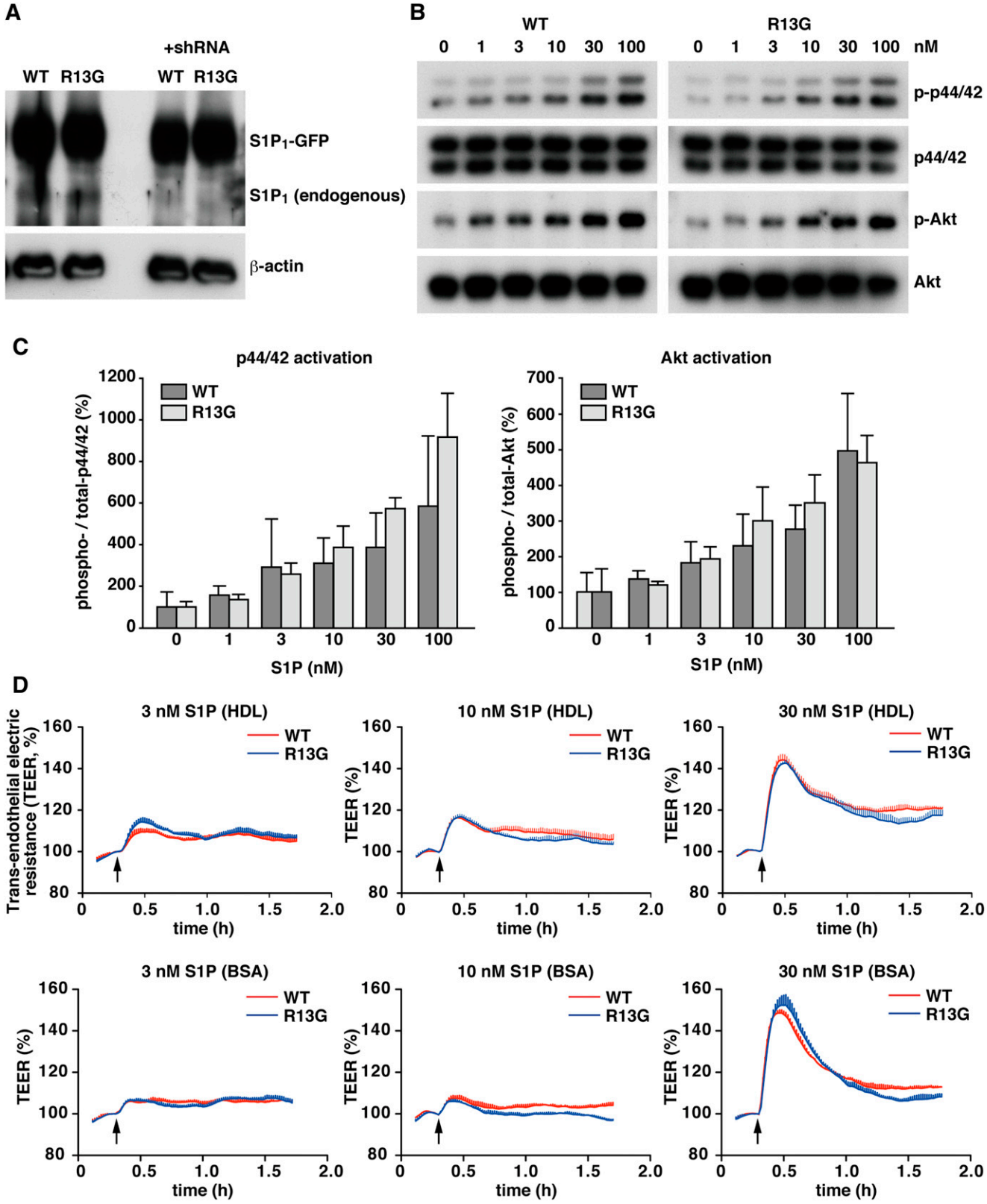

Fig. 6. Functional comparison between WT $S1P_1$ and R13G mutant in HUVECs. HUVECs were transduced with lentivirus vectors for the expression of GFP-tagged $S1P_1$ or R13G mutant together with a vector for endogenous $S1P_1$-specifc shRNA. A: Western blot analysis was performed to check the overexpression of WT $S1P_1$ and R13G and the suppression of endogenous $S1P_1$ by shRNA. B: The cells were starved for 3 h and stimulated with the indicated concentrations of HDL-bound S1P for 5 min. Total cell lysates were prepared and subjected to Western blot analyses for the activation of p44/42 MAPK and Akt. C: Densitometric analysis of (B) by the National Institutes of Health ImageJ program is shown. Data represent the mean + SD (n = 3). D: The cells were starved for 3 h and stimulated with the indicated concentrations of HDL-bound (upper panel) or BSA-bound (lower panel) S1P. The changes in TEER were monitored in an ECIS θ system (Applied Biophysics). Data are the mean ± SEM (n = 3) and are representative of three independent experiments with the same tendency.

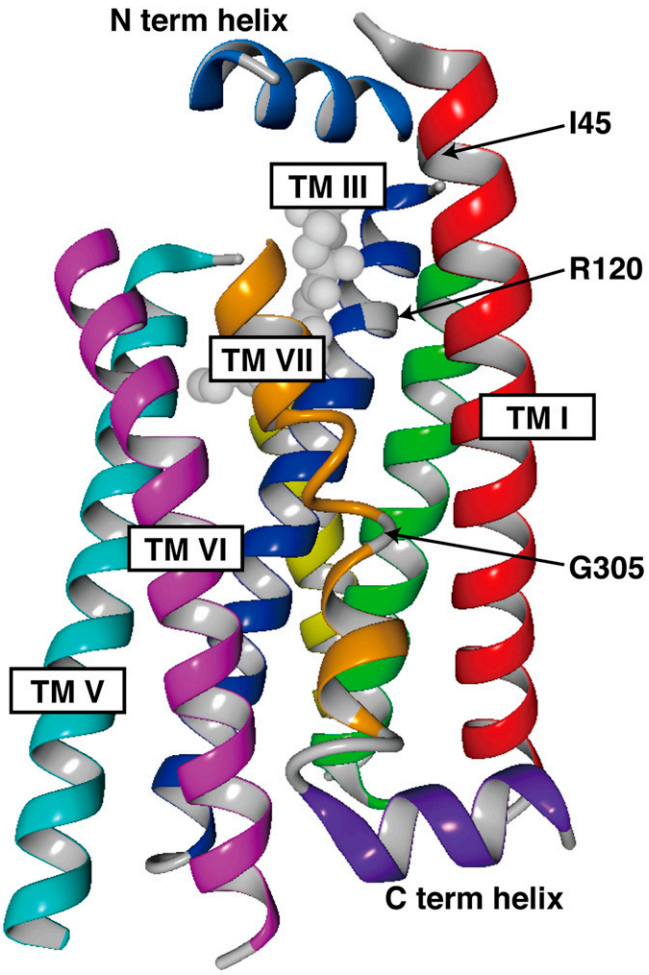

Fig. 7. Three-dimensional structure of $S1P_1$. Three-dimensional structure of human $S1P_1$ is illustrated by using a program (YASARA) based on the crystal structure of $S1P_1$ (Protein Data Bank number 3V2Y). Only α-helixes and a cocrystalized antagonist (ML056) are shown. Arrows denote the positions of Ile^{45}, Arg^{120}, and Gly^{305}. TM, transmembrane.

unfavorable for the stability of α-helixes and has the second lowest helix propensity next to proline (47). Gly^{305} to Cys mutation may constrain this flexible loop and interfere with ligand-induced conformational changes required for endocytosis. Another possibility is that Cys^{305} might create an additional disulfide bond between another Cys residue. There are four cysteine residues within the transmembrane helixes of $S1P_1$ [Cys^{56}, Cys^{57} (helix I), Cys^{206} (helix V), and Cys^{268} (helix VI)]. These cysteine residues could be potential intra-molecule bonding partners. It is also possible that Cys^{305} could make an inter-molecule disulfide bond with a cysteine residue of a transmembrane domain of another molecule, because many GPCRs are shown to homo/hetero-dimerize (48).

In addition to the functional analysis of 14 nonsynonymous mutations of $S1P_1$ found in the NHLBI GO ESP database, we performed a sequencing analysis of the *S1PR1* gene in the cardiovascular disease cohort and found that R13G shows a significantly higher incidence than that observed in the NHLBI GO ESP (3.58% versus 1.24%). Moreover, the number of patients with multi-vessel obstructions was significantly lower in the R13G group in comparison with the age-, gender-, and risk factor-matched control group, which suggests that the R13G mutation might reduce the severity of coronary atherosclerotic obstructions. Although we tried to clarify functional differences of the R13G mutant in an in vitro study using HUVECs, we did not find any differences compared with WT $S1P_1$, at least in the assay systems we performed. However, atherosclerotic arterial obstructions develop through complex interactions between endothelial cells, smooth muscle cells, macrophages, and lymphocytes. Therefore, it is possible that the R13G mutant might be functionally different in some of these cell types or might affect interaction between these cell types. To establish physiological/clinical significance of the R13G mutation, further case-control studies should be conducted in a cardiovascular disease cohort, as well as other disease cohorts. In vitro characterization of the R13G mutant in various cell types will also be necessary.

In summary, findings in this study suggest that individual variations in $S1P_1$ may influence cardiovascular/immune functions as well as drug sensitivity and, therefore, infer differential risks for cardiovascular and autoimmune diseases as well as response to S1P receptor modulatory drugs. Sufficiently powered prospective cohort studies should be conducted to validate possible relationships between individual variations in the $S1P_1$ receptor and specific diseases/drug sensitivity.

The authors thank the Lipidomics Shared Resources at the Medical University of South Carolina for the measurement of S1P concentration and Dr. DiLorenzo for her help in the TEER measurements.

REFERENCES

1. Blaho, V. A., and T. Hla. 2011. Regulation of mammalian physiology, development, and disease by the sphingosine 1-phosphate and lysophosphatidic acid receptors. *Chem. Rev.* **111:** 6299–6320.
2. Obinata, H., and T. Hla. 2012. Sphingosine 1-phosphate in coagulation and inflammation. *Semin. Immunopathol.* **34:** 73–91.
3. Cyster, J. G., and S. R. Schwab. 2012. Sphingosine-1-phosphate and lymphocyte egress from lymphoid organs. *Annu. Rev. Immunol.* **30:** 69–94.
4. Murata, N., K. Sato, J. Kon, H. Tomura, M. Yanagita, A. Kuwabara, M. Ui, and F. Okajima. 2000. Interaction of sphingosine 1-phosphate with plasma components, including lipoproteins, regulates the lipid receptor-mediated actions. *Biochem. J.* **352:** 809–815.
5. Christoffersen, C., H. Obinata, S. B. Kumaraswamy, S. Galvani, J. Ahnström, M. Sevvana, C. Egerer-Sieber, Y. A. Muller, T. Hla, L. B. Nielsen, et al. 2011. Endothelium-protective sphingosine-1-phosphate provided by HDL-associated apolipoprotein M. *Proc. Natl. Acad. Sci. USA.* **108:** 9613–9618.
6. Jung, B., H. Obinata, S. Galvani, K. Mendelson, B-S. Ding, A. Skoura, B. Kinzel, V. Brinkmann, S. Rafii, T. Evans, et al. 2012. Flow-regulated endothelial S1P receptor-1 signaling sustains vascular development. *Dev. Cell.* **23:** 600–610.
7. Gaengel, K., C. Niaudet, K. Hagikura, B. Laviña, B. L. Siemsen, L. Muhl, J. J. Hofmann, L. Ebarasi, S. Nyström, S. Rymo, et al. 2012. The sphingosine-1-phosphate receptor S1PR1 restricts sprouting angiogenesis by regulating the interplay between VE-cadherin and VEGFR2. *Dev. Cell.* **23:** 587–599. [Erratum. 2012. *Dev. Cell.* **23:** 1264.]
8. Ben Shoham, A., G. Malkinson, S. Krief, Y. Shwartz, Y. Ely, N. Ferrara, K. Yaniv, and E. Zelzer. 2012. S1P1 inhibits sprouting angiogenesis during vascular development. *Development.* **139:** 3859–3869.

9. Lee, M. J., S. Thangada, K. P. Claffey, N. Ancellin, C. H. Liu, M. Kluk, M. Volpi, R. I. Sha'afi, and T. Hla. 1999. Vascular endothelial cell adherens junction assembly and morphogenesis induced by sphingosine-1-phosphate. *Cell.* **99:** 301–312.
10. Sanchez, T., T. Estrada-Hernandez, J. H. Paik, M. T. Wu, K. Venkataraman, V. Brinkmann, K. Claffey, and T. Hla. 2003. Phosphorylation and action of the immunomodulator FTY720 inhibits vascular endothelial cell growth factor-induced vascular permeability. *J. Biol. Chem.* **278:** 47281–47290.
11. Camerer, E., J. B. Regard, I. Cornelissen, Y. Srinivasan, D. N. Duong, D. Palmer, T. H. Pham, J. S. Wong, R. Pappu, and S. R. Coughlin. 2009. Sphingosine-1-phosphate in the plasma compartment regulates basal and inflammation-induced vascular leak in mice. *J. Clin. Invest.* **119:** 1871–1879.
12. Nofer, J. R., M. van der Giet, M. Tölle, I. Wolinska, K. von Wnuck Lipinski, H. A. Baba, U. J. Tietge, A. Gödecke, I. Ishii, B. Kleuser, et al. 2004. HDL induces NO-dependent vasorelaxation via the lysophospholipid receptor S1P3. *J. Clin. Invest.* **113:** 569–581.
13. Argraves, K. M., and W. S. Argraves. 2007. HDL serves as a S1P signaling platform mediating a multitude of cardiovascular effects. *J. Lipid Res.* **48:** 2325–2333.
14. Okajima, F., K. Sato, and T. Kimura. 2009. Anti-atherogenic actions of high-density lipoprotein through sphingosine 1-phosphate receptors and scavenger receptor class B type I. *Endocr. J.* **56:** 317–334.
15. Potì, F., M. Simoni, and J. R. Nofer. 2014. Atheroprotective role of high density lipoprotein (HDL)-associated sphingosine 1-phosphate (S1P). *Cardiovasc. Res.* **103:** 395–404.
16. Hla, T., K. Venkataraman, and J. Michaud. 2008. The vascular S1P gradient-cellular sources and biological significance. *Biochim. Biophys. Acta.* **1781:** 477–482.
17. Hanson, M. A., C. B. Roth, E. Jo, M. T. Griffith, F. L. Scott, G. Reinhart, H. Desale, B. Clemons, S. M. Cahalan, S. C. Schuerer, et al. 2012. Crystal structure of a lipid G protein-coupled receptor. *Science.* **335:** 851–855.
18. Rosen, H., R. C. Stevens, M. Hanson, E. Roberts, and M. B. A. Oldstone. 2013. Sphingosine-1-phosphate and its receptors: structure, signaling, and influence. *Annu. Rev. Biochem.* **82:** 637–662.
19. Lee, M. J., M. Evans, and T. Hla. 1996. The inducible G protein-coupled receptor edg-1 signals via the G(i)/mitogen-activated protein kinase pathway. *J. Biol. Chem.* **271:** 11272–11279.
20. Windh, R. T., M. J. Lee, T. Hla, S. An, A. J. Barr, and D. R. Manning. 1999. Differential coupling of the sphingosine 1-phosphate receptors Edg-1, Edg-3, and H218/Edg-5 to the G(i), G(q), and G(12) families of heterotrimeric G proteins. *J. Biol. Chem.* **274:** 27351–27358.
21. Lee, M. J., S. Thangada, J. H. Paik, G. P. Sapkota, N. Ancellin, S. S. Chae, M. Wu, M. Morales-Ruiz, W. C. Sessa, D. R. Alessi, et al. 2001. Akt-mediated phosphorylation of the G protein-coupled receptor EDG-1 is required for endothelial cell chemotaxis. *Mol. Cell.* **8:** 693–704.
22. Watterson, K. R., E. Johnston, C. Chalmers, A. Pronin, S. J. Cook, J. L. Benovic, and T. M. Palmer. 2002. Dual regulation of EDG1/S1P(1) receptor phosphorylation and internalization by protein kinase C and G-protein-coupled receptor kinase 2. *J. Biol. Chem.* **277:** 5767–5777.
23. Liu, C. H., S. Thangada, M. J. Lee, J. R. Van Brocklyn, S. Spiegel, and T. Hla. 1999. Ligand-induced trafficking of the sphingosine-1-phosphate receptor EDG-1. *Mol. Biol. Cell.* **10:** 1179–1190.
24. Thangada, S., K. M. Khanna, V. A. Blaho, M. L. Oo, D. S. Im, C. Guo, L. Lefrancois, and T. Hla. 2010. Cell-surface residence of sphingosine 1-phosphate receptor 1 on lymphocytes determines lymphocyte egress kinetics. *J. Exp. Med.* **207:** 1475–1483.
25. Oo, M. L., S. H. Chang, S. Thangada, M. T. Wu, K. Rezaul, V. Blaho, S. I. Hwang, D. K. Han, and T. Hla. 2011. Engagement of $S1P_1$-degradative mechanisms leads to vascular leak in mice. *J. Clin. Invest.* **121:** 2290–2300.
26. Garris, C. S., L. Wu, S. Acharya, A. Arac, V. A. Blaho, Y. Huang, B. S. Moon, R. C. Axtell, P. P. Ho, G. K. Steinberg, et al. 2013. Defective sphingosine 1-phosphate receptor 1 (S1P1) phosphorylation exacerbates TH17-mediated autoimmune neuroinflammation. *Nat. Immunol.* **14:** 1166–1172.
27. Brinkmann, V., A. Billich, T. Baumruker, P. Heining, R. Schmouder, G. Francis, S. Aradhye, and P. Burtin. 2010. Fingolimod (FTY720): discovery and development of an oral drug to treat multiple sclerosis. *Nat. Rev. Drug Discov.* **9:** 883–897.
28. Obinata, H., and T. Hla. 2012. Fine-tuning S1P therapeutics. *Chem. Biol.* **19:** 1080–1082.
29. Bigaud, M., D. Guerini, A. Billich, F. Bassilana, and V. Brinkmann. 2014. Second generation S1P pathway modulators: research strategies and clinical developments. *Biochim. Biophys. Acta.* **1841:** 745–758.
30. Oo, M. L., S. Thangada, M. T. Wu, C. H. Liu, T. L. Macdonald, K. R. Lynch, C. Y. Lin, and T. Hla. 2007. Immunosuppressive and anti-angiogenic sphingosine 1-phosphate receptor-1 agonists induce ubiquitinylation and proteasomal degradation of the receptor. *J. Biol. Chem.* **282:** 9082–9089.
31. Sun, X., S. F. Ma, M. S. Wade, C. Flores, M. Pino-Yanes, J. Morita, C. Ober, R. Kittles, A. N. Husain, J. G. Ford, et al. 2010. Functional variants of the sphingosine-1-phosphate receptor 1 gene associate with asthma susceptibility. *J. Allergy Clin. Immunol.* **126:** 241–249.
32. NHLBI GO Exome Sequencing Project (ESP). Exome Variant Server, Seattle, WA. Accessed June 2012, at http://evs.gs.washington.edu/EVS/.
33. Obinata, H., and T. Hla. 2012. Assessment of sphingosine-1-phosphate activity in biological samples by receptor internalization and adherens junction formation. *Methods Mol. Biol.* **874:** 69–76.
34. Aratake, Y., T. Okuno, T. Matsunobu, K. Saeki, R. Takayanagi, S. Furuya, and T. Yokomizo. 2012. Helix 8 of leukotriene B4 receptor 1 inhibits ligand-induced internalization. *FASEB J.* **26:** 4068–4078.
35. Arehart, E., J. Stitham, F. W. Asselbergs, K. Douville, T. MacKenzie, K. M. Fetalvero, S. Gleim, Z. Kasza, Y. Rao, L. Martel, et al. 2008. Acceleration of cardiovascular disease by a dysfunctional prostacyclin receptor mutation: potential implications for cyclooxygenase-2 inhibition. *Circ. Res.* **102:** 986–993.
36. Havel, R. J., H. A. Eder, and J. H. Bragdon. 1955. The distribution and chemical composition of ultracentrifugally separated lipoproteins in human serum. *J. Clin. Invest.* **34:** 1345–1353.
37. Bielawski, J., J. S. Pierce, J. Snider, B. Rembiesa, Z. M. Szulc, and A. Bielawska. 2009. Comprehensive quantitative analysis of bioactive sphingolipids by high-performance liquid chromatography-tandem mass spectrometry. *Methods Mol. Biol.* **579:** 443–467.
38. Parrill, A. L., D. Wang, D. L. Bautista, J. R. Van Brocklyn, Z. Lorincz, D. J. Fischer, D. L. Baker, K. Liliom, S. Spiegel, and G. Tigyi. 2000. Identification of Edg1 receptor residues that recognize sphingosine 1-phosphate. *J. Biol. Chem.* **275:** 39379–39384.
39. Koyrakh, L., M. I. Roman, V. Brinkmann, and K. Wickman. 2005. The heart rate decrease caused by acute FTY720 administration is mediated by the G protein-gated potassium channel IKACh. *Am. J. Transplant.* **5:** 529–536.
40. Garcia, J. G., F. Liu, A. D. Verin, A. Birukova, M. A. Dechert, W. T. Gerthoffer, J. R. Bamberg, and D. English. 2001. Sphingosine 1-phosphate promotes endothelial cell barrier integrity by Edg-dependent cytoskeletal rearrangement. *J. Clin. Invest.* **108:** 689–701.
41. Liu, Y., R. Wada, T. Yamashita, Y. Mi, C. X. Deng, J. P. Hobson, H. M. Rosenfeldt, V. E. Nava, S. S. Chae, M. J. Lee, et al. 2000. Edg-1, the G protein-coupled receptor for sphingosine-1-phosphate, is essential for vascular maturation. *J. Clin. Invest.* **106:** 951–961.
42. Allende, M. L., T. Yamashita, and R. L. Proia. 2003. G protein-coupled receptor S1P1 acts within endothelial cells to regulate vascular maturation. *Blood.* **102:** 3665–3667.
43. Helenius, A. 1994. How N-linked oligosaccharides affect glycoprotein folding in the endoplasmic reticulum. *Mol. Biol. Cell.* **5:** 253–265.
44. Wheatley, M., D. Wootten, M. T. Conner, J. Simms, R. Kendrick, R. T. Logan, D. R. Poyner, and J. Barwell. 2012. Lifting the lid on GPCRs: the role of extracellular loops. *Br. J. Pharmacol.* **165:** 1688–1703.
45. Kohno, T., A. Wada, and Y. Igarashi. 2002. N-glycans of sphingosine 1-phosphate receptor Edg-1 regulate ligand-induced receptor internalization. *FASEB J.* **16:** 983–992.
46. Soto, A. G., and J. Trejo. 2010. N-linked glycosylation of protease-activated receptor-1 second extracellular loop: a critical determinant for ligand-induced receptor activaiton and internalization. *J. Biol. Chem.* **285:** 18781–18793.
47. Pace, C. N., and J. M. Scholtz. 1998. A helix propensity scale based on experimental studies of peptides and proteins. *Biophys. J.* **75:** 422–427.
48. Audet, M., and M. Bouvier. 2012. Restructuring G protein-coupled receptor activation. *Cell.* **151:** 14–23.